TE and TM Modes in Cylindrical Metallic Structures Filled with Bianisotropic Material

Roberto D. Graglia, *Senior Member, IEEE*, Maria S. Sarto, *Member, IEEE*, and Piergiorgio L. E. Uslenghi, *Fellow, IEEE*

Abstract— **Modal propagation is studied for metallic circular waveguides, coaxial cables and sectoral waveguides filled with linear bianisotropic material. By representing the material constitutive tensors in cylindrical coordinates, the conditions under which TE and TM modal decoupling occurs are obtained, and second-order differential equations for the longitudinal field components are derived. Though the TE and TM longitudinal field components are expressible in terms of hypergeometric functions, a complete numerical solution scheme is, in general, more convenient. Conventional application of finite elements renders the differential problem numerically equivalent to a generalized eigenvalue matrix problem, whose solution yields the dispersion relation and cutoff frequencies of the waveguides together with the eigenfields expression. The effects one can obtain by varying the various coefficients of the constitutive tensors are illustrated by several numerical results.**

I. Introduction

In RECENT years there has been a growing interest in new materials for special applications in applied electromagnetics; these materials (e.g., chiral materials, biased ferrites, ceramics, etc.) are all special cases of the most general linear medium having bianisotropic constitutive relations [1]–[3]. Since additional applications are likely to occur as a consequence of the introduction of novel synthetic materials, it is important to predict the electromagnetic behavior of a general bianisotropic medium; for example, the dispersion relation of this medium has been studied in [4], applications to planar layered structures have been considered in [5] while planar bianisotropic waveguiding structures have been considered only very recently in [6], [7]. To study guided propagation in bianisotropic media one could use the kDB system introduced in [1], [2]; however, no real advantage is gained by describing the fields using the flux density vectors $\boldsymbol{D}$ and $\boldsymbol{B}$ instead of the electric ($\boldsymbol{E}$) and magnetic ($\boldsymbol{H}$) field vectors, since the $\boldsymbol{E}$ and $\boldsymbol{H}$ fields are needed when imposing the boundary conditions.

In this paper, we determine the conditions under which guided propagation in circular, coaxial and sectoral metallic waveguides filled with bianisotropic material can be described in terms of TE and TM modes. In Section II we discuss the general conditions for the existence of TE and TM modes in cylindrical coordinates; these conditions vary with the coordinate system and, in fact, the conditions which apply when rectangular coordinates are employed have been obtained in [8].

In Section III we derive the expression of the modal field components in terms of the longitudinal ones for the circular, coaxial and sectoral waveguides, when TE-TM decoupling occurs. The solutions obtained with a homogeneous filler are then discussed in some detail and the possibility of modifying the single-mode bandwidth of a circular waveguide is illustrated in the simpler case of an anisotropic filler. Section III also shows that the longitudinal electric and magnetic field components are the eigensolutions of second-order differential equations, subject to appropriate boundary conditions. Special attention is devoted to the conditions to be used to numerically deal with the circular waveguide problem.

Finally, several results are discussed in Section IV to illustrate the effects on the waveguide dispersion diagrams due to different choices of the constitutive parameters. The parameters in the examples are assumed to be frequency independent only for sake of simplicity, since the method and the numerical code presented here are directly applicable to frequency-dispersive media. Some of the results pertaining to the circular coaxial waveguide have been presented in [9].

II. General Conditions for the Existence of TE and TM Modes in Cylindrical Coordinates

Let us consider a waveguiding structure whose axis is the z axis of a cylindrical reference frame (ρ, ϕ, z). The waveguide is filled with bianisotropic material characterized by the frequency-domain constitutive relations

$$\begin{aligned} \boldsymbol{D} &= \varepsilon_o \underline{\varepsilon} \boldsymbol{E} + \frac{1}{c_o} \underline{\xi} \boldsymbol{H} \\ \boldsymbol{B} &= \mu_o \underline{\mu} \boldsymbol{H} - \frac{1}{c_o} \underline{\eta} \boldsymbol{E} \end{aligned} \tag{1}$$

where μ_o and ε_o are the free-space magnetic permeability and electric permittivity, respectively, $c_o = 1/\sqrt{\mu_o \varepsilon_o}$ is the velocity of light in free space while, in cylindrical coordinates, the four dimensionless constitutive tensors $\underline{\varepsilon}, \underline{\mu}, \underline{\xi}$ and $\underline{\eta}$ are represented by 3×3 matrices of the type $\underline{\varepsilon} = \{\varepsilon_{i\ell}; i, \ell = 1, 2, 3\}_{\rho\phi z}$, where $\varepsilon_{i\ell}$ are constants. The assumption of constant tensor coefficients in cylindrical coordinates is required here not to violate the circular symmetry of the problems

Manuscript received December 18, 1995; revised April 19, 1996. This work was supported in part by the Italian National Research Council (CNR) under Grant 95.01552.07.

R. D. Graglia is with the Dipartimento di Elettronica, Politecnico di Torino, Corso Duca degli Abruzzi 24, 10129 Torino, Italy.

M. S. Sarto is with the Dipartimento di Ingegneria Elettrica, Università di Roma "La Sapienza," Via Eudossiana 18, 00184 Roma, Italy.

P. L. E. Uslenghi is with the Department of Electrical Engineering and Computer Science, University of Illinois at Chicago, Chicago, IL 60607-7053 USA.

Publisher Item Identifier S 0018-9480(96)05649-9.

we intend to study. However, this assumption permits one to consider an inhomogeneous coaxial layered filler obtained, for example, by rolling up thin layers of different homogeneous bianisotropic material; this layered structure can be used, for instance, as a filler of a coaxial waveguide. In other words, we point out that the bianisotropic materials considered here are, in general, inhomogeneous; in fact, the dyadic

$$(\hat{\boldsymbol{\rho}}\,\hat{\boldsymbol{\phi}}\,\hat{\boldsymbol{z}})\begin{pmatrix}\varepsilon_{11} & \varepsilon_{12} & \varepsilon_{13}\\ \varepsilon_{21} & \varepsilon_{22} & \varepsilon_{23}\\ \varepsilon_{31} & \varepsilon_{32} & \varepsilon_{33}\end{pmatrix}_{\rho\phi z}\begin{pmatrix}\hat{\boldsymbol{\rho}}\\ \hat{\boldsymbol{\phi}}\\ \hat{\boldsymbol{z}}\end{pmatrix} \tag{2}$$

is, in general, a function of space coordinates, even if the coefficients $\varepsilon_{i\ell}$ are constant. The bianisotropic medium is lossless if $\underline{\varepsilon} = \underline{\varepsilon}^{+}, \underline{\mu} = \underline{\mu}^{+}$ and $\underline{\eta} = -\underline{\xi}^{+}$, where the superscript + denotes a transpose and complex conjugate [1, chap. 1].

The modal electric and magnetic fields may be written as

$$\begin{aligned}\boldsymbol{E}(\rho,\phi,z) &= \boldsymbol{e}(\rho)\exp(jm\phi)\Phi(z)\exp(j\omega t)\\ \boldsymbol{H}(\rho,\phi,z) &= Y_o\boldsymbol{h}(\rho)\exp(jm\phi)\Phi(z)\exp(j\omega t)\end{aligned} \tag{3}$$

with

$$\Phi(z) = \exp(-j\beta k_o z) \tag{4}$$

and where $k_o = \omega/c_o, \beta$ is the normalized longitudinal propagation constant, $Z_o = Y_o^{-1} = \sqrt{\mu_o/\varepsilon_o}$ is the free-space impedance and m is an integer whenever periodicity of all field components of 2π radians in ϕ is required. In the following, the time-dependence factor $\exp(j\omega t)$ is omitted and

$$\boldsymbol{e}(\rho) = e_\rho(\rho)\hat{\boldsymbol{\rho}} + e_\phi(\rho)\hat{\boldsymbol{\phi}} + e_z(\rho)\hat{\boldsymbol{z}} \tag{5}$$

with a similar expression for $\boldsymbol{h}(\rho)$.

By use of Maxwell's equations one can express the transverse field components in terms of the longitudinal components e_z, h_z and their derivatives. In turns, the components e_z and h_z are solutions of two *coupled* second-order differential equations with variable coefficients, that are difficult to solve in the general case. The fact that, in general, these equations are coupled shows that the waveguiding structure supports hybrid modes.

The conditions under which these equations decouple, leading to superposition of TE and TM fields, are determined as follows. First of all one has to distinguish the parent equation for TM modes from the TE parent equation; this is done by considering the two coupled differential equations in the limit of isotropic material (where the two equations decouple). Then, one systematically equates to zero all the coefficients of e_z and its derivatives in the TE parent equation, and all the coefficients of h_z and its derivatives in the TM parent equation. This process, though simple in principle, is quite long and complex in practice; it results in the following theorem:

If $\varepsilon_{11}, \varepsilon_{22}$ and $(\varepsilon_{11}\varepsilon_{22} - \varepsilon_{12}\varepsilon_{21})$ are nonzero, then TE–TM decoupling occurs if and only if

$$\varepsilon_{12}\varepsilon_{31} = \varepsilon_{11}\varepsilon_{32} \tag{6}$$

$$\varepsilon_{21}\varepsilon_{13} = \varepsilon_{11}\varepsilon_{23} \tag{7}$$

$$\underline{\xi} = \begin{pmatrix}0 & \xi_{12} & 0\\ -\xi_{12} & 0 & \xi_{23}\\ 0 & -\xi_{23} & 0\end{pmatrix}_{\rho\phi z} \tag{8}$$

$$\underline{\eta} = \begin{pmatrix}0 & \eta_{12} & 0\\ -\eta_{12} & 0 & \eta_{23}\\ 0 & -\eta_{23} & 0\end{pmatrix}_{\rho\phi z} \tag{9}$$

$$\underline{\mu} = \alpha\begin{pmatrix}\varepsilon_{11} & \varepsilon_{21} & \varepsilon_{31}\\ \varepsilon_{12} & \varepsilon_{22} & \varepsilon_{32}\\ \varepsilon_{13} & \varepsilon_{23} & \dfrac{\mu_{33}}{\alpha}\end{pmatrix}_{\rho\phi z} \tag{10}$$

where α is any finite nonzero constant. Notice that the matrices (8) and (9) representing the tensors $\boldsymbol{\xi}$ and $\boldsymbol{\eta}$ are singular and immediately prove that a chiral waveguiding structure cannot support TE and TM modes [10]. Conditions (6) and (7) constrain to zero the coefficients $\{2,3\}$ and $\{3,2\}$ of the inverse of $\underline{\varepsilon}$ and $\underline{\mu}$. Moreover, if the waveguiding region comprises the axis $\rho = 0$, then the material constitutive tensors in cartesian coordinates must be ϕ-independent at $\rho = 0$. This is a feasibility condition which, together with conditions (6)–(10), immediately yields

$$\begin{aligned}&\varepsilon_{11} = \varepsilon_{22}\\ &\varepsilon_{21} = -\varepsilon_{12}\\ &\varepsilon_{13} = \varepsilon_{23} = \varepsilon_{31} = \varepsilon_{32} = 0\\ &\xi_{23} = \eta_{23} = 0.\end{aligned} \tag{11}$$

A bianisotropic material which complies with conditions (11) (and (6)–(10)) is homogeneous; in fact, for example, the matrix representing the tensor $\underline{\varepsilon}$ is

$$\underline{\varepsilon} = \begin{pmatrix}\varepsilon_{11} & \varepsilon_{12} & 0\\ -\varepsilon_{12} & \varepsilon_{11} & 0\\ 0 & 0 & \varepsilon_{33}\end{pmatrix} \tag{12}$$

both in circular and cartesian (x,y,z) coordinates, with $\hat{\boldsymbol{x}} = \hat{\boldsymbol{\rho}}(\phi = 0)$ and $\hat{\boldsymbol{y}} = \hat{\boldsymbol{\rho}}(\phi = \pi/2)$.

III. TE and TM Modes in Circular Bianisotropic Waveguides

In the following, we study several bianisotropic waveguiding structures under conditions (6)–(10).

A. Field Components

By setting

$$k_o\rho = r \tag{13}$$

the TM and TE differential equations may be written as follows:

$$\begin{aligned}&e_z'' + \frac{e_z'}{r} + e_z\left(\gamma^2 - \frac{m^2}{r^2}\right)\\ &\quad + je_z'\left[\frac{m}{r}\,\frac{(\varepsilon_{12}+\varepsilon_{21})}{\varepsilon_{11}} + v + u\right]\\ &\quad - e_z\left[\frac{m^2}{r^2}\,\frac{(\varepsilon_{22}-\varepsilon_{11})}{\varepsilon_{11}} + \frac{m}{r}\,\frac{(u\varepsilon_{12}+v\varepsilon_{21})}{\varepsilon_{11}}\right.\\ &\quad \left. + v\left(u - \frac{j}{r}\right) - \gamma^2 s_e\right] = 0\end{aligned} \tag{14}$$

$$h_z'' + \frac{h_z'}{r} + h_z\left(\gamma^2 - \frac{m^2}{r^2}\right) + jh_z'\left[\frac{m}{r}\frac{(\mu_{12}+\mu_{21})}{\mu_{11}} + u + v\right] - h_z\left[\frac{m^2}{r^2}\frac{(\mu_{22}-\mu_{11})}{\mu_{11}} + \frac{m}{r}\frac{(v\mu_{12}+u\mu_{21})}{\mu_{11}} + u\left(v - \frac{j}{r}\right) - \gamma^2 s_h\right] = 0 \quad (15)$$

with

$$\gamma^2 = \delta - (\beta - \eta_{12})(\beta - \xi_{12}) \quad (16)$$

$$\delta = \alpha(\varepsilon_{11}\varepsilon_{22} - \varepsilon_{12}\varepsilon_{21}) = \frac{1}{\alpha}(\mu_{11}\mu_{22} - \mu_{12}\mu_{21}) \quad (17)$$

$$u = \xi_{23} - (\beta - \xi_{12})\frac{\varepsilon_{31}}{\varepsilon_{11}} = \xi_{23} - (\beta - \xi_{12})\frac{\mu_{13}}{\mu_{11}} \quad (18)$$

$$v = \eta_{23} - (\beta - \eta_{12})\frac{\varepsilon_{13}}{\varepsilon_{11}} = \eta_{23} - (\beta - \eta_{12})\frac{\mu_{31}}{\mu_{11}} \quad (19)$$

$$s_e = \frac{\varepsilon_{33} - \varepsilon_{11}}{\varepsilon_{11}} - \frac{\varepsilon_{13}\varepsilon_{31}}{\varepsilon_{11}^2} \quad (20)$$

$$s_h = \frac{\mu_{33} - \mu_{11}}{\mu_{11}} - \frac{\mu_{13}\mu_{31}}{\mu_{11}^2}. \quad (21)$$

Equations (14)–(21) do agree with the duality principle, that in our case reads as follows:

$$\boldsymbol{e} \Longrightarrow \boldsymbol{h}, \quad \boldsymbol{h} \Longrightarrow -\boldsymbol{e}, \quad \varepsilon_{ij} \Longleftrightarrow \mu_{ij}, \quad \eta_{ij} \Longleftrightarrow \xi_{ij}, \quad \alpha \Longleftrightarrow 1/\alpha, \quad u \Longleftrightarrow v, \quad s_e \Longleftrightarrow s_h. \quad (22)$$

In the case of isotropic material, (14), (15) reduce to the usual Bessel differential equation $f'' + f'/r + f(p^2\gamma^2 - m^2/r^2) = 0$, with $p = 1, \gamma^2 = (\varepsilon\mu - \beta^2)$ and where $f = e_z, h_z$ for TM and TE mode, respectively. As is well known, the solution of this classical problem can be expressed by a linear combination of the functions $J_m(\gamma r)$ and $Y_m(\gamma r)$, which are the Bessel functions of order m of the first and second kind, respectively; in the isotropic case γ is the normalized radial propagation constant. A Bessel differential equation as above is also obtained from (14) and (15) for a homogeneous medium (i.e., under conditions (11), which imply $u = v = 0$). The solution of these simpler bianisotropic cases is a linear combination of the functions $J_m(p\gamma r)$ and $Y_m(p\gamma r)$, with $p^2 = \varepsilon_{33}/\varepsilon_{11}, \mu_{33}/\mu_{11}$ for TM and TE modes, respectively (see, for example, the discussion relative to the results of Fig. 2 later on).

To see a conceptually simpler application of the previous result, let us consider a circular waveguide filled with a homogeneous anisotropic material ($\boldsymbol{\eta} = \boldsymbol{\xi} = \mathbf{0}$) with diagonal $\underline{\boldsymbol{\mu}} = \text{diag}\,[\mu_a, \mu_a, \mu_{33}]$ and $\underline{\varepsilon} = \varepsilon_a \boldsymbol{I}$, where $\boldsymbol{I}$ is the identity matrix and where μ_a, μ_{33} and ε_a are real. Here, conditions (11) are satisfied as a special case, with $p = 1, \sqrt{\mu_{33}/\mu_a}$ for TM and TE mode, respectively; while (16) yields $\gamma^2 + \beta^2 = \varepsilon_a\mu_a$. In this case, the dispersion diagrams of all the TM modes are equal to those relative to an isotropic waveguide with $\varepsilon\mu = \varepsilon_a\mu_a$ (since $h_z = 0$ for TM modes); conversely, the cutoff frequencies of the TE modes are $1/p$ times those of the isotropic waveguide though, for very large value of frequency (where $h_z \approx 0$ or, equivalently, $\gamma \approx 0$), one still gets an asymptotic value of $\beta^2 = \varepsilon_a\mu_a$. The TE_{11} single-mode bandwidth increases for increasing value of μ_{33}/μ_a and for $\mu_{33}/\mu_a > 1$ is wider than that of the isotropic waveguide; for $\sqrt{\mu_{33}/\mu_a} \lesssim 1.841/2.405$ the first mode supported by the waveguide is the TM_{01}. Obviously, the TE_{11} single-mode bandwidth can also be modified by varying the $\varepsilon_{33}/\varepsilon_a$ ratio of a diagonal electric premittivity tensor $\underline{\varepsilon} = \text{diag}\,[\varepsilon_a, \varepsilon_a, \varepsilon_{33}]$. For all these homogeneous anisotropic waveguides the topography of the transverse modal-fields is equal to that of an isotropic waveguide with $\varepsilon\mu = \varepsilon_a\mu_a$ [see (25)]. The same result can be shown to hold in cartesian coordinates for rectangular homogeneous waveguides.

By returning to the most general case, it is important to observe that, as opposed to what happens for isotropic materials, (14) and (15) yield, in general, a different couple of second-order differential equations by changing m into $(-m)$. The differential equations become even in m iff

$$\varepsilon_{12} + \varepsilon_{21} = 0, \qquad \varepsilon_{12}(u - v) = 0. \quad (23)$$

These conditions are satisfied independently from the value of β if conditions (11) hold, or if

$$\varepsilon_{12} + \varepsilon_{21} = 0, \qquad \varepsilon_{23} + \varepsilon_{32} = 0, \qquad \varepsilon_{12}(\xi_{23} - \eta_{23}) = \varepsilon_{23}(\xi_{12} - \eta_{12}). \quad (24)$$

By use of (6) and (7), one readily proves that conditions (24) imply $\varepsilon_{13} = \varepsilon_{31}$. In particular, note that the differential equations become even in m for $\varepsilon_{12} = \varepsilon_{21} = 0$, a condition which implies $\varepsilon_{23} = \varepsilon_{32} = 0$ (and $\mu_{12} = \mu_{21} = \mu_{23} = \mu_{32} = 0$).

Once the longitudinal components are known, the transverse field components are easily obtained from Maxwell's equations; for TM modes one has

$$\begin{bmatrix} e_\rho \\ e_\phi \\ h_\rho \\ h_\phi \end{bmatrix}_{\text{TM}} = \frac{1}{\gamma^2}\begin{bmatrix} v(\beta - \xi_{12}) - \gamma^2\dfrac{\varepsilon_{13}}{\varepsilon_{11}} \\ \dfrac{m}{r}(\beta - \xi_{12}) \\ -v\varepsilon_{21} - \dfrac{m}{r}\varepsilon_{22} \\ v\varepsilon_{11} + \dfrac{m}{r}\varepsilon_{12} \end{bmatrix} e_z - \frac{j}{\gamma^2}\begin{bmatrix} \beta - \xi_{12} \\ 0 \\ -\varepsilon_{21} \\ \varepsilon_{11} \end{bmatrix} e_z' \quad (25)$$

whereas the TE transverse components are obtained by duality from (25). In general, the longitudinal components of $\boldsymbol{D}$ and $\boldsymbol{B}$ are different from zero; for example, for TM modes, the constitutive equations yield

$$B_{z_{\text{TM}}} = \frac{m}{c_o r}\left[\frac{v}{\gamma^2}(\beta - \xi_{12}) - \frac{\varepsilon_{13}}{\varepsilon_{11}}\right] e_z. \quad (26)$$

B. Boundary Conditions

By setting to zero the electric field components e_ϕ and e_z on the metal waveguide boundary, one obtains the boundary

conditions for (14) and (15)

$$e_z = 0 \tag{27}$$

$$h'_z = -j\left(u + \frac{m}{r}\frac{\mu_{12}}{\mu_{11}}\right)h_z. \tag{28}$$

Notice that the boundary condition (28) (for TE modes) is, in general, β-dependent; in case of isotropic material, or for $u = 0$ and $\mu_{12} = 0$ ($\varepsilon_{21} = 0$), the previous expressions simplify to the usual ones.

The above boundary conditions suffice to solve the coaxial waveguide problem whereas, to find the modes of a circular waveguide, a different condition at $r = 0$ is required to ensure bounded field solutions. In the particular case of isotropic material, use of this boundary condition eliminates from the Bessel problem the solutions $Y_m(\gamma r)$. Furthermore, an acceptable solution under a physical point of view must yield fields ($\boldsymbol{D}, \boldsymbol{B}, \boldsymbol{E}$, and $\boldsymbol{H}$ fields) having the correct degree of continuity on the axis; this results in a second condition at $r = 0$, which is a continuity condition that can not be used to integrate the differential equation, but is used to accept or reject *a posteriori* the mathematical modal-solutions of the differential problem. As a matter of fact, as we will see further on, the continuity condition is automatically satisfied under conditions (11) (homogeneous medium); therefore these are the only conditions required to correctly formulate, also under a physical point of view, the circular waveguide problem[1]. For azimuthal index $m = 0$, an analysis of the terms of order $(1/r)$ in (14), (15) leads to the boundary conditions $e'_z + jve_z = 0$ and $h'_z + juh_z = 0$; in this case the regularity of the fields on the axis $r = 0$ (continuity condition) requires the vanishing of the radial and azimuthal field components at $r = 0$. Conversely, for $m \neq 0$, the regularity conditions are obtained after setting $e_z = re'_z$ and $h_z = rh'_z$ for small values of r (boundary conditions), in order to first ensure bounded field solutions on the polar axis. The conditions at $r = 0$ are reported in Table I. Notice that, for $m = \pm 1$, the regularity of the fields on the axis does not necessarily imply the vanishing of the transverse field components at $r = 0$. Indeed, in cartesian coordinates ($\hat{\boldsymbol{x}} = \hat{\boldsymbol{\rho}}(\phi = 0), \hat{\boldsymbol{y}} = \hat{\boldsymbol{\rho}}(\phi = \pi/2)$), the $\mathrm{TM}_{m=\pm 1}$ fields on the polar axis are:

$$\begin{bmatrix}\boldsymbol{E}\\ \boldsymbol{H}\end{bmatrix}_{\mathrm{TM}} = -\frac{\hat{\boldsymbol{x}} + jm\hat{\boldsymbol{y}}}{\gamma^2}\begin{bmatrix} j(\beta - \xi_{12}) \\ Y_o(m\varepsilon_{11} + j\varepsilon_{12})\end{bmatrix}\Phi(z)e'_z, \quad m = \pm 1 \tag{29}$$

while the $\mathrm{TE}_{m=\pm 1}$ fields are given by duality.

Observe that under conditions (11) (which imply $u = v = 0$), the continuity conditions of Table I are satisfied by arbitrary values of the longitudinal fields (e_z, h_z) for $m = 0$ while, for $m = \pm 1$, one always has $e'_z = a_e$ and $h'_z = a_h$ at $r = 0$. Once again, under conditions (11), it turns out that the solutions of the homogeneous circular waveguide problem are given by the Bessel functions $J_m(p\gamma r)$ which, at $r = 0$, satisfy the boundary condition and naturally agree with the continuity condition. On the contrary, if we were to assume that, unphysically, conditions (11) are not satisfied, the mathematical solutions of the differential problem do not fulfil the continuity condition (for example, one finds that the $m = 0$ modes violate the continuity condition).

[1] According to conds. (11), a medium having constant tensor coefficients in cylindrical coordinates on the whole circular waveguide cross-section must be homogeneous. The same condition is independently obtained here by considering the continuity condition at $\rho = 0$ for an inhomogeneous medium.

TABLE I

IN ORDER TO FIND THE MODES OF A CIRCULAR WAVEGUIDE, CONDITIONS AT $r = 0$ ARE REQUIRED TO ENSURE FIELD SOLUTIONS WHICH ARE BOUNDED AND CONTINUOUS WHILE CROSSING THE POLAR AXIS IN THE TABLE, b.c. MEANS BOUNDARY CONDITION, WHILE c.c. MEANS CONTINUITY CONDITION FOR $m = \pm 1, a_e, a_h$ DENOTE TWO (ARBITRARY) CONSTANTS. FOR AN ISOTROPIC MEDIUM, THE CONDITIONS REPORTED IN THE TABLE REDUCE TO THE USUAL CONDITIONS SATISFIED BY THE BESSEL FUNCTIONS $J_m(\gamma r)$

Regularity conditions at r=0 for TM_m and TE_m modes in a circular bianisotropic waveguide			
	$m = 0$	$m = \pm 1$	$\lvert m\rvert \geq 2$
b.c	$e'_z + jve_z = 0$	$e_z = 0$	$e_z = 0$
c c	$\varepsilon_{13}e_z = \varepsilon_{23}e_z = = \eta_{23}e_z = 0$	$e'_z = \begin{cases} a_e & \text{for } \varepsilon_{22} - \varepsilon_{11} = jm(\varepsilon_{12} + \varepsilon_{21}) \\ 0 & \text{for } \varepsilon_{22} - \varepsilon_{11} \neq jm(\varepsilon_{12} + \varepsilon_{21}) \end{cases}$	$e'_z = 0$
b.c.	$h'_z + juh_z = 0$	$h_z = 0$	$h_z = 0$
c.c.	$\mu_{13}h_z = \mu_{23}h_z = = \xi_{23}h_z = 0$	$h'_z = \begin{cases} a_h & \text{for } \mu_{22} - \mu_{11} = jm(\mu_{12} + \mu_{21}) \\ 0 & \text{for } \mu_{22} - \mu_{11} \neq jm(\mu_{12} + \mu_{21}) \end{cases}$	$h'_z = 0$

In general (i.e., for $\xi_{12} \neq 0, \eta_{12} \neq 0$ and/or $\varepsilon_{12} \neq 0$), the transverse field components of a circular waveguide filled with a homogeneous bianisotropic material are, for given values of p, β, and γ, different from the ones observed in the isotropic case having normalized radial propagation constant equal to $p\gamma$, even if the longitudinal components are given by the same Bessel functions of the first kind [see, for example, (25)].

Obviously, the bianisotropic filler of a coaxial waveguide does not need to comply with conditions (11); in this case the filler can also be realized as a coaxial layered (inhomogeneous) structure and one has more degrees of freedom since ξ_{23} and η_{23} are not constrained to zero.

C. TEB Modes in Coaxial Waveguides

The results derived previously are not valid for $\gamma = 0$, where (16) yields

$$\beta = \frac{\eta_{12} + \xi_{12} \mp \sqrt{(\eta_{12} - \xi_{12})^2 + 4\delta}}{2} \tag{30}$$

with $\beta = \mp\sqrt{\mu\varepsilon}$ for isotropic material. However, this case is simpler than the general one and is readily solved in an analytic way, thereby proving the possible existence of a TEB mode in a coaxial waveguide, that is to say a mode having a zero longitudinal component for both the $\boldsymbol{e}$ and $\boldsymbol{B}$ fields. In fact, for coaxial waveguides at $\gamma = 0$, the boundary conditions and Maxwell's equations might be satisfied by eigenfields having the following form:

$$\boldsymbol{e} = k_o\frac{\exp(-jur)}{r}\Phi(z)\hat{\boldsymbol{\rho}}$$

$$\boldsymbol{B} = k_o\frac{\exp(-jur)}{r}\Phi(z)\frac{\beta}{c_o}\hat{\boldsymbol{\phi}} \tag{31}$$

though one has to distinguish between the two cases $u = 0$ and $u \neq 0$ to assess the possible existence of this mode and to express the $\boldsymbol{h}$ and $\boldsymbol{D}$ fields.

1) For $u = 0$ (e.g., isotropic or homogeneous bianisotropic material), there always exists a TEB mode which is also TEM. In this case one has $\exp(-jur) = 1$ and

$$\boldsymbol{h} = \frac{k_o}{\beta - \xi_{12}}\Phi(z)\frac{\varepsilon_{11}\hat{\boldsymbol{\phi}} - \varepsilon_{21}\hat{\boldsymbol{\rho}}}{r}$$
$$\boldsymbol{D} = \frac{\beta k_o \varepsilon_o}{\beta - \xi_{12}}\Phi(z)\frac{\varepsilon_{11}\hat{\boldsymbol{\rho}} + \varepsilon_{21}\hat{\boldsymbol{\phi}}}{r}. \tag{32}$$

2) For $u \neq 0$ (and $\gamma = 0$), there exists a TEB mode only if

$$\mu_{33} = \alpha\varepsilon_{33} \tag{33}$$
$$\varepsilon_{11}\varepsilon_{33} = \varepsilon_{13}\varepsilon_{31}. \tag{34}$$

In this case the possibility of considering isotropic or homogeneous bianisotropic materials is excluded by condition (34), and the TEB mode is not transverse magnetic (i.e., it is a TE mode); the $\boldsymbol{h}$ and $\boldsymbol{D}$ fields are[2]

$$\boldsymbol{h} = \mathcal{M}\left[\frac{\varepsilon_{11}}{r}\hat{\boldsymbol{\phi}} - \left(\frac{\varepsilon_{21}}{r} + \varepsilon_{31}\right)\hat{\boldsymbol{\rho}} + \varepsilon_{11}\hat{\boldsymbol{z}}\right]$$
$$\boldsymbol{D} = \varepsilon_o\beta\mathcal{M}\left[\frac{\varepsilon_{11}}{r}\hat{\boldsymbol{\rho}} + \left(\frac{\varepsilon_{21}}{r} + \varepsilon_{31} + \varepsilon_{11}\frac{u}{\beta}\right)\hat{\boldsymbol{\phi}} - \frac{\varepsilon_{11}}{r}\frac{u}{\beta}\hat{\boldsymbol{z}}\right] \tag{35}$$

with:

$$\mathcal{M} = k_o\frac{\exp(-jur)}{\beta - \xi_{12}}\Phi(z). \tag{36}$$

Since $\hat{\boldsymbol{z}} \cdot \boldsymbol{\nabla} \times \boldsymbol{e} = 0$ [see (31)], one can define a potential function Ψ, in the transverse plane $z = \text{const.}$, such that $\boldsymbol{e} = -\boldsymbol{\nabla}_t\Psi$ (with $\boldsymbol{\nabla}_t = \boldsymbol{\nabla} - \hat{\boldsymbol{z}}\partial/\partial z$). For a coaxial waveguide of inner radius $\rho = b$ and outer radius $\rho = a$, the voltage difference $V_u(z)$ between the inner and outer conductor is expressed in terms of sine and cosine integrals

$$V_u(z) = \Phi(z)[\mathrm{Ci}(uk_o\rho) - j\mathrm{Si}(uk_o\rho)]_{\rho=b}^{\rho=a} \tag{37}$$

with $V_o(z) = \Phi(z)\ln(a/b)$ for $u = 0$. The current $I_u(z)$ flowing in the inner conductor is easily evaluated by use of Maxwell–Ampère's law. In particular, for $u = 0$, this current is simply given by the circulation of $\boldsymbol{H} = \boldsymbol{h}/Z_o$, since $\hat{\boldsymbol{z}} \cdot \boldsymbol{D} = 0$. The current $I_u(z)$ has the following general expression

$$I_u(z) = \frac{2\pi Y_o\varepsilon_{11}}{(\beta - \xi_{12})}\exp(-juk_ob)\Phi(z) \tag{38}$$

which, for $u = 0$, reads $I_o(z) = 2\pi Y_o\varepsilon_{11}\Phi(z)/(\beta - \xi_{12})$.

The impedance of the cable for the TEB mode is $Z_c = V_u/I_u$ which, for $u = 0$, yields

$$Z_c = \frac{V_o}{I_o} = Z_o\frac{(\beta - \xi_{12})}{2\pi\varepsilon_{11}}\ln(a/b) = k_o\frac{(\beta - \xi_{12})}{2\pi\omega\varepsilon_o\varepsilon_{11}}\ln(a/b). \tag{39}$$

In the limit of isotropic material, (39) yields the well-known result $Z_c = \frac{Z}{2\pi}\ln(a/b)$, with $Z = Z_o\sqrt{\mu/\varepsilon}$.

[2] Notice that (20), (21) under conditions (33), (34) yield $s_e = s_h = -1$; in this particular case, the coefficient multiplying γ^2 in both (14) and (15) does vanish.

D. Sectoral Waveguide

Let us now consider a sectoral waveguiding structure whose perfectly conducting walls bound the region $\{b \leq \rho \leq a; 0 \leq \phi \leq \phi_o\}$, with $\phi_o \leq 2\pi$. The sectoral waveguide is obtained by filling with perfectly conducting material the angular region ϕ: $\{\phi_o - 2\pi \leq \phi \leq 0\}$ of a coaxial waveguide with outer radius $\rho = a$ and inner radius $\rho = b > 0$; the case $b = 0$ is excluded because of the complexity of the boundary conditions at the edge of the wedge.

Even under conditions (6)–(10), the modes supported by this structure are, in general, hybrid modes. TM and TE modes may appear only when it is possible to combine the two modes of index $\pm m$ of the coaxial waveguide into a single mode, so to satisfy the boundary conditions on the metal septum. Hence, TE and TM modes may exist only under the supplemental conditions (24); the differential equations (14) and (15) relative to these modes become even in m.

In fact, it is easily found that the sectoral waveguide supports TM modes only when conditions (24) are valid; the TM eigenfields have the following form (the fields vanish for $m = 0$):

$$\boldsymbol{e} = \Phi(z)[(e_{\rho_s}\hat{\boldsymbol{\rho}} + e_{z_s}\hat{\boldsymbol{z}})\sin m\phi - jm\hat{\boldsymbol{\phi}}e_{\phi_c}\cos m\phi]$$
$$\boldsymbol{h} = \Phi(z)[(h_{\rho_s}\boldsymbol{\rho} + h_{\phi_s}\hat{\boldsymbol{\phi}})\sin m\phi + jm(h_{\rho_c}\hat{\boldsymbol{\rho}} + h_{\phi_c}\hat{\boldsymbol{\phi}})\cos m\phi]$$
$$m = n\frac{\pi}{\phi_o} \quad \text{with } n \geq 1 \text{ and integer} \tag{40}$$

with

$$\begin{bmatrix} e_{\rho_s} \\ e_{\phi_c} \\ h_{\rho_s} \\ h_{\phi_s} \\ h_{\rho_c} \\ h_{\phi_c} \end{bmatrix}_{\mathrm{TM}} = \frac{1}{\gamma^2}\begin{bmatrix} v(\beta - \xi_{12}) - \gamma^2\frac{\varepsilon_{13}}{\varepsilon_{11}} \\ \frac{(\beta - \xi_{12})}{r} \\ -v\varepsilon_{21} \\ v\varepsilon_{11} \\ \frac{\varepsilon_{22}}{r} \\ -\frac{\varepsilon_{12}}{r} \end{bmatrix} e_{z_s} - \frac{j}{\gamma^2}\begin{bmatrix} \beta - \xi_{12} \\ 0 \\ -\varepsilon_{21} \\ \varepsilon_{11} \\ 0 \\ 0 \end{bmatrix} e'_{z_s} \tag{41}$$

where the subscript s (c) refers to terms proportional to $\sin m\phi$ $(\cos m\phi)$.

Conversely, the sectoral waveguide supports TE modes only if $\varepsilon_{12} = \varepsilon_{21} = 0$ (which is a particular case of conditions (24), with $\varepsilon_{23} = \varepsilon_{32} = 0$ and $\mu_{12} = \mu_{21} = \mu_{23} = \mu_{32} = 0$). In this case, the TE eigenfields have the following form (valid also for $m = 0$):

$$\boldsymbol{e} = \Phi(z)[\hat{\boldsymbol{\phi}}e_{\phi_c}\cos m\phi + jme_{\rho_s}\hat{\boldsymbol{\rho}}\sin m\phi]$$
$$\boldsymbol{h} = \Phi(z)[(h_{\rho_c}\hat{\boldsymbol{\rho}} + h_{z_c}\hat{\boldsymbol{z}})\cos m\phi + jmh_{\phi_s}\hat{\boldsymbol{\phi}}\sin m\phi]$$
$$m = n\frac{\pi}{\phi_o} \quad \text{with } n \geq 0 \text{ and integer} \tag{42}$$

with:

$$\begin{bmatrix} e_{\rho_s} \\ e_{\phi_c} \\ h_{\phi_s} \\ h_{\rho_c} \end{bmatrix}_{\mathrm{TE}} = \frac{1}{\gamma^2} \begin{bmatrix} \dfrac{\mu_{22}}{r} \\ -u\mu_{11} \\ \dfrac{(\beta - \eta_{12})}{r} \\ u(\beta - \eta_{12}) - \gamma^2 \dfrac{\mu_{13}}{\mu_{11}} \end{bmatrix} h_{z_c} - \frac{j}{\gamma^2} \begin{bmatrix} 0 \\ -\mu_{11} \\ 0 \\ \beta - \eta_{12} \end{bmatrix} h'_{z_c}. \quad (43)$$

The previous eigenfields fulfil the boundary conditions on the metal septum; to solve (14), (15) one has to further set $e_{z_s} = 0$ and $h'_{z_c} = -juh_{z_c}$ at $r = k_o a, k_o b$.

IV. Numerical Results

Our differential problem is easily solved numerically by applying the finite element method [11]. Along the waveguide radial axis n nodes are defined as the extreme points of $(n-1)$ adjacent subintervals. The first node is located at $r = k_o b$, the last one at $r = k_o a$, a and b being the outer and inner waveguide radius, respectively, ($b = 0$ for a circular waveguide).

By introducing Hermite expansion functions on each subinterval, one has to solve for $2n$ unknowns; these are the values of the longitudinal field component (e_z or h_z) and of its first derivative at each of the n nodes [12]. A Galerkin testing procedure is then applied to obtain a discretized problem in matrix form. Notice that a similar approach has also been used in the numerical solution of integral equations in [13], though a delta sampling procedure was there used to test the equations. Cubic Hermite expansion functions were chosen here to allow the strong enforcement of the boundary conditions; as opposite to what happens when using linear expansion functions (elements), which would require to implement the boundary conditions of our problem in a weak form.

For any given value of the azimuthal index m, the differential problem assumes the following discretized form:

$$\underline{\boldsymbol{A}}\boldsymbol{x} + \beta\underline{\boldsymbol{B}}\boldsymbol{x} + \beta^2\underline{\boldsymbol{C}}\boldsymbol{x} = 0 \quad (44)$$

where $\underline{\boldsymbol{A}}, \underline{\boldsymbol{B}}$ and $\underline{\boldsymbol{C}}$ are square sparse matrices having bandwidth equal to six; $\boldsymbol{x}$ is the unknown column vector (eigenvector), and β is the unknown normalized longitudinal propagation constant (eigenvalue). By setting $\boldsymbol{y} = \beta\boldsymbol{x}$, problem (44) is reduced to the following *linear* generalized eigenvalue problem (of doubled size):

$$\begin{bmatrix} \underline{\boldsymbol{A}} & \underline{0} \\ \underline{0} & -\underline{\boldsymbol{I}} \end{bmatrix} \begin{bmatrix} \boldsymbol{x} \\ \boldsymbol{y} \end{bmatrix} + \beta \begin{bmatrix} \underline{\boldsymbol{B}} & \underline{\boldsymbol{C}} \\ \underline{\boldsymbol{I}} & \underline{0} \end{bmatrix} \begin{bmatrix} \boldsymbol{x} \\ \boldsymbol{y} \end{bmatrix} = \begin{bmatrix} 0 \\ 0 \end{bmatrix} \quad (45)$$

where $\underline{0}$ is the null matrix; problem (45) is numerically solved by use of standard library routines.

All the results reported in this section have been obtained with $n = 28$ (i.e., 56 unknowns) and are relative to $\underline{\varepsilon} = 4\underline{\boldsymbol{I}}$ and $\underline{\boldsymbol{\mu}} = \underline{\boldsymbol{I}}$. This choice of parameters renders the differential equations even in m [see (24)], a condition which simplifies the graphical presentation of the results. Furthermore, for sake of simplicity, the parameters of the examples discussed in this Section are assumed to be frequency independent, even though our numerical code can directly deal with frequency-dispersive media.

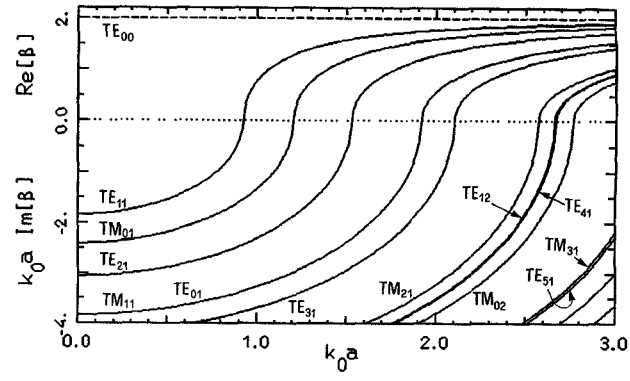

Fig. 1. Dispersion diagram of the first modes of a circular waveguide of radius a, filled with isotropic material $\underline{\varepsilon} = 4\underline{\boldsymbol{I}}, \underline{\boldsymbol{\mu}} = \underline{\boldsymbol{I}}, \underline{\boldsymbol{\xi}} = \underline{\boldsymbol{\eta}} = \underline{0}$. The exact analytical results (solid-lines) are compared with the dashed-line results, obtained numerically.

In Fig. 1 we report the dispersion diagram of the first modes of a circular isotropic waveguide ($\underline{\boldsymbol{\xi}} = \underline{\boldsymbol{\eta}} = \underline{0}$) of radius a. The figure reports the value of the normalized longitudinal constant β when the modes are above cutoff and the value of $k_o a\ \mathrm{Im}[\beta]$ when modes are below cutoff. The dashed-line results, obtained numerically, are compared with the analytical results reported by solid-lines. Notice that our numerical results are undistinguishable from the analytical ones; the only difference is due to the presence of one unphysical solution of the TE equation for $m = 0$. In the figure, this solution is labeled as TE_{00} and yields $\beta = 2\forall(k_o a)$, which is the β-value given by (30) for $\gamma = 0$. Since the numerically obtained TE_{00} eigenfield is constant along the waveguide radial axis ($h_z = \mathrm{const.}$), all the TE_{00} transverse field components are zero. Hence, the TE_{00} solution can be regarded as a static solution and must be discarded. However, notice that this is a correct solution of (15), (28) for $m = 0$ and $\gamma = 0$; that is to say for β as given by (30).

Fig. 2 reports the numerically obtained dispersion diagrams for the first two modes (TE_{11} and TM_{01}) of a circular waveguide of radius a, filled with the homogeneous lossless bianisotropic material $\xi_{23} = \eta_{23} = 0, \xi_{12} = -\eta_{12} = js$; for $s = 1.2$, 0.6 and 0 (isotropic case). For this choice of parameters γ^2 is an even function of β and the figure reports only the value of β relative to progressive waves ($\beta = \beta_p$), since $\beta_r = -\beta_p$ for regressive waves. Fig. 2 does not report the TE_{00} unphysical solutions; for $s \neq 0$ the h_z field component of these numerical solutions is not constant in ρ, but it does yield zero transverse field components of $\boldsymbol{E}$ and $\boldsymbol{H}$, as in the isotropic case $s = 0$. The TE_{00} dispersion diagrams always exhibit a constant value of β for all $k_o a$, with β given by (30); for the other modes, the dispersion diagrams for large values of $k_o a$ asymptotically tend to this value of β. Notice also that the dispersion diagrams of Fig. 2 coincide with those relative to an isotropic material with $\varepsilon\mu = \gamma^2 + \beta^2 = \delta - \eta_{12}\xi_{12} = 4 - s^2$. In fact, in the case of Fig. 2 one has $p = 1$ so that, for example, the two TE_{11} modal

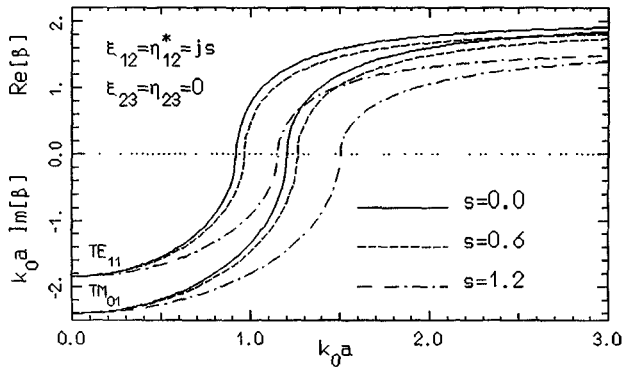

Fig. 2. TE_{11} and TM_{01} numerically obtained dispersion diagrams for a circular waveguide of radius a, filled with bianisotropic material $\underline{\varepsilon} = 4\underline{I}, \underline{\mu} = \underline{I}, \xi_{23} = \eta_{23} = 0, \xi_{12} = -\eta_{12} = js$: for $s = 1.2$, 0.6 and 0 (isotropic case). The dispersion diagrams in the figure coincide with those relative to an isotropic material with $\varepsilon\mu = \gamma^2 + \beta^2 = \delta - \eta_{12}\xi_{12} = 4 - s^2$.

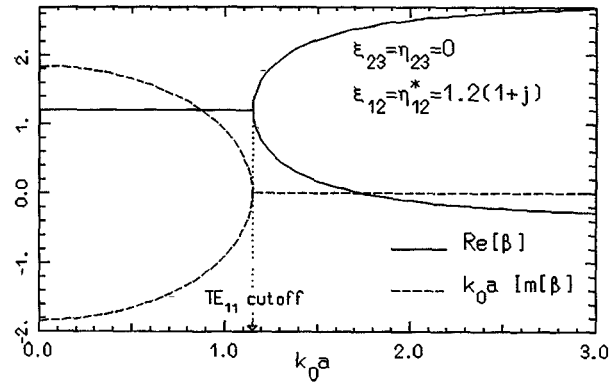

Fig. 3. Numerically obtained dispersion diagram of the first mode (TE_{11}) of a circular waveguide of radius a, filled with bianisotropic material $\underline{\varepsilon} = 4\underline{I}, \underline{\mu} = \underline{I}, \xi_{23} = \eta_{23} = 0, \xi_{12} = \eta_{12}^* = 1.2\,(1+j)$. The figure reports the results relative to both the regressive and progressive mode. Notice how β has a constant real part equal to 1.2 below cutoff.

solutions for the longitudinal magnetic field can be written as follows:

$$H_z = -j\gamma^2 Y_o \Phi(z) J_1(\gamma r) \begin{pmatrix} \cos\phi \\ \sin\phi \end{pmatrix}. \tag{46}$$

The corresponding TE_{11} modal electric fields are

$$\boldsymbol{E} = \Phi(z)\left[\hat{\boldsymbol{\phi}} J_1'(\gamma r) \begin{pmatrix} \cos\phi \\ \sin\phi \end{pmatrix} \pm \hat{\boldsymbol{\rho}} \frac{J_1(\gamma r)}{r} \begin{pmatrix} \sin\phi \\ \cos\phi \end{pmatrix}\right] \tag{47}$$

while $\boldsymbol{H}_t = Y_o(\beta + js)\hat{\boldsymbol{z}} \times \boldsymbol{E}$ is the transverse magnetic field. Thus, the TE_{11} transverse electric and magnetic fields are in quadrature for $\beta = 0$ and $s \neq 0$ while, as well known, $\boldsymbol{H}_t = 0$ in the isotropic ($s = 0$) case at $\beta = 0$.

Fig. 3 reports the TE_{11} dispersion diagram of a circular waveguide of radius a, filled with the homogeneous material $\xi_{23} = \eta_{23} = 0, \xi_{12} = \eta_{12}^* = s(1 + j)$, where $s = 1.2$ and the superscript * denotes a complex conjugate. In this case γ^2 is an even function of $(\beta - s)$, and one finds that β has a constant real part equal to s below cutoff. The figure reports the results for both the regressive and progressive mode; asymptotically, for large value of $k_o a$, one has $\beta = -0.4$, 2.8 for regressive and progressive mode, respectively (in fact, (30) yields $\beta = s \mp \sqrt{4 - s^2}$).

Fig. 4 report the dispersion diagrams of coaxial bianisotropic waveguides of outer radius $\rho = a$, inner radius $\rho = b$ with $a/b = 12.2$. The coefficients of $\underline{\eta}$ and $\underline{\xi}$ where choosen so to obtain $\beta_r = -\beta_p$ for regressive modes, where $\beta = \beta_p$ for progressive waves. Fig. 4(a) shows the results for the first four modes obtained with a homogeneous filler $\xi_{23} = \eta_{23} = 0$ (i.e., $u = 0$), $\xi_{12} = -\eta_{12} = js$; for $s = 1.2$ and 0 (isotropic case). In this case the TEB mode is a TEM mode with impedance $Z_c \simeq 75[\Omega], (60 - j45)[\Omega]$ for $s = 0$ and 1.2, respectively. Since the coefficients of the constitutive tensors and the cable impedance must be real at $\omega = 0$, the results of Fig. 4 are not significant at $\omega = 0$; obviously, as said previously, one can not neglect frequency-dispersion toward zero frequency. Fig. 4(b) reports the dispersion diagrams of the first three modes of a coaxial cable with $u \neq 0$ (inhomogeneous filler); these results were obtained by setting $\xi_{12} = \xi_{23} = -\eta_{12} = -\eta_{23} = j1.2$.

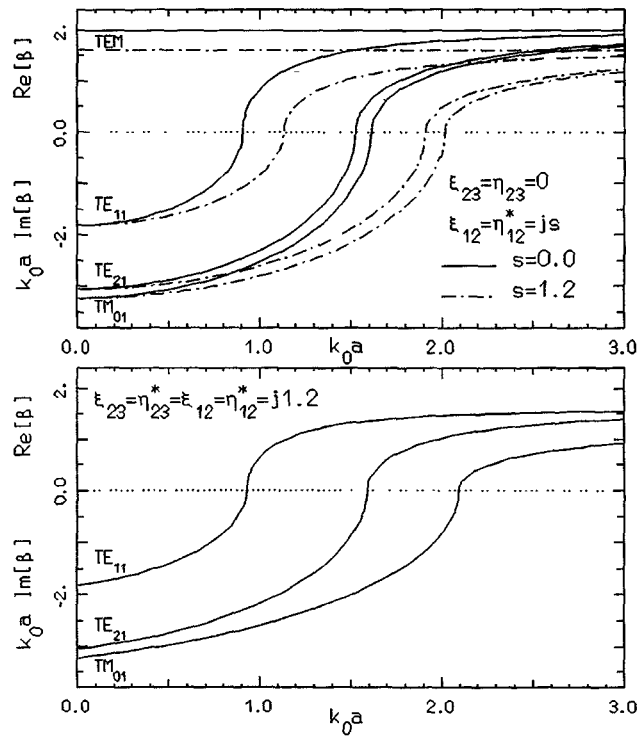

Fig. 4. Numerically obtained dispersion diagrams for coaxial waveguides having outer radius $\rho = a$, inner radius $\rho = b$, with $a/b = 12.2$: the waveguide bianisotropic filler has $\underline{\varepsilon} = 4\underline{I}, \underline{\mu} = \underline{I}$. (a) at top, the figure reports the results obtained with $\xi_{23} = \eta_{23} = 0, \xi_{12} = -\eta_{12} = js$; for $s = 1.2$ and 0 (isotropic case). (b) at bottom, the dispersion diagrams obtained by setting $\xi_{12} = \xi_{23} = -\eta_{12} = -\eta_{23} = j1.2$ are shown; in this case the TEM mode is not supported and the first mode of the coaxial cable is the TE_{11}.

Since this structure does not support a TEB mode (see Section III-C) the first mode of the coaxial cable is the TE_{11}. The results of Fig. 4 illustrate the effects on the dispersion diagrams due to different choices of the $\underline{\eta}$ and $\underline{\xi}$ parameters. For diagonal $\underline{\varepsilon}$ and $\underline{\mu}$ it is sufficient to choose $\xi_{23} \neq 0$ to eliminate the TEM mode of the coaxial cable; for $\xi_{23} = 0$ the impedance of the TEM mode is modified by choosing an imaginary value for ξ_{12}, while the cable remains lossless for $\eta_{23} = -\xi_{23}^*, \eta_{12} = -\xi_{12}^*$.

V. Conclusion

The conditions under which TE and TM modal decoupling occurs in metallic circular waveguides, coaxial cables and sectoral waveguides filled with bianisotropic material have been presented. For the different waveguides considered, the modal (TE and TM) transverse-field components have been expressed in terms of the longitudinal modal components; these, in turn, are the eigensolutions of second-order differential equations, subject to appropriate boundary conditions. The boundary conditions have been derived, with special attention to those useful to (numerically) deal with the circular waveguide problem. Since our differential model has been derived by working in the frequency-domain, the results presented are directly applicable to consider frequency-dispersive media.

The differential problem has been numerically solved by applying the Finite Element method and by expanding the modal longitudinal field components in terms of Hermite cubic functions. The dispersion relations together with the waveguide eigenfield expressions were numerically obtained as solution of linear generalized eigenvalue problems. Several numerical results have been reported to illustrate the different effects one can obtain by varying the various tensor coefficients of the waveguide bianisotropic filler.

References

[1] J. A. Kong, *Theory of Electromagnetic Waves*. New York: Wiley, 1975.

[2] ——, *Electromagnetic Wave Theory*. New York: Wiley, 1986.

[3] T. H. O'Dell, *The Electrodynamics of Magnetoelectric Media*. New York: North-Holland, 1970.

[4] R. D. Graglia, P. L. E. Uslenghi, and R. E. Zich, "Dispersion relation for bianisotropic materials and its symmetry properties," *IEEE Trans. Antennas Propagat.*, vol. 39, no. 1, pp. 83–90, Jan. 1991.

[5] ——, "Reflection and transmission for planar structures of bianisotropic media," *Electromagnetics*, vol. 11, no. 2, pp. 193–208, 1991.

[6] H.-Y. Yang and P. L. E. Uslenghi, "Planar bianisotropic waveguides," *Radio Sci.*, vol. 28, pp. 919–927, 1993.

[7] J. D. Ali, "Theory of parallel-plate waveguides partially filled with magnetoelectric materials," Ph.D. dissertation, Univ. of Illinois at Chicago, 1994.

[8] P. L. E. Uslenghi, "TE-TM decoupling for guided propagation in bianisotropic media," *IEEE Trans. Antennas Propagat.*, accepted.

[9] R. D. Graglia, M. S. Sarto, and P. L. E. Uslenghi, "Theory of coaxial cable filled with bianisotropic material," in *Proc. PIER Symp.*, Seattle, WA, July 1995, p. 287.

[10] I. V. Lindell, A. H. Sihvola, S. A. Tretyakov, and A. J. Viitanen, *Electromagnetic Waves in Chiral and Bi-Isotropic Media*. Norwood, MA: Artech House, 1994.

[11] O. C. Zienkiewicz and R. L. Taylor, *The Finite Element Method*, 4th ed. New York: McGraw-Hill, 1989.

[12] R. Vichnetvetsky, *Computer Methods for Partial Differential Equations*, vol. 1. Englewood Cliffs, N. J.: Prentice-Hall, 1981.

[13] R. D. Graglia, P. L. E. Uslenghi, R. Vitiello, and U. D'Elia, "Electromagnetic scattering for oblique incidence on impedance bodies of revolution," *IEEE Trans. Antennas Propagat.*, vol. 43, no. 1, pp. 11–26, Jan. 1995.

Roberto D. Graglia (S'83–M'83–SM'90) was born in Turin, Italy, on July 6, 1955. He received the Laurea degee (summa cum laude) in electronic engineering from the Polytechnic of Turin in 1979, and the Ph.D. degree in electrical engineering and computer science from the University of Illinois at Chicago in 1983.

In 1980 to 1981, he was a Research Engineer at CSELT, Italy, where he conducted research on microstrip circuits. In 1981 to 1983, he was a Teaching and Research Assistant at the University of Illinois, Chicago; and then, since 1992, a Researcher with the Italian National Research Council (CNR). In 1991 and in 1993 he was Associate Visiting Professor at the University of Illinois, Chicago. He is currently Associate Professor of Electrical Engineering at the Polytechnic of Turin, Italy, and Associate Editor of the IEEE Transactions on Antennas And Propagation. His areas of interest are numerical methods for high and low frequency electromagnetics, theoretical and computational aspects of scattering and interactions with complex media, waveguides, antennas, electromagnetic compatibility, and low–frequency phenomena.

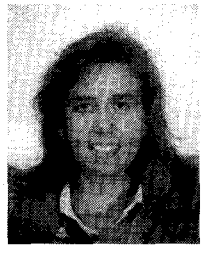

Maria S. Sarto (M'93) was born in Rome, Italy, on May 20, 1968. She received the Laurea degree in electrical engineering from the University of Rome "La Sapienza" in 1992.

Since 1994, she has been Researcher at the University of Rome. Her research activity is mainly in the field of electromagnetic compatibility, and includes fast transient analysis and modeling of multiconductor networks, field propagation.

Piergiorgio L. E. Uslenghi (SM'70–F'90) was born in Turin, Italy, in 1937. He received the doctorate in electrical engineering from the Polytechnic of Turin, and the M. S. and Ph.D. degrees in physics from the University of Michigan, Ann Arbor, in 1960, 1964, and 1967, respectively.

He has been an Assistant Professor at the Polytechnic of Turin (1961), Associate Research Engineer at Conductron Corporation, Ann Arbor, MI (1962 to 1963), and a Research Physicist at the Radiation Laboratory of the University of Michigan (1963 to 1970). In 1970, he joined the University of Illinois, Chicago, where he held a number of positions, including Founder and first Director of the Communications Laboratory (1976 to 1978), Founder and Director of the Electromagnetics Laboratory (1991 to present), Professor of Electrical Engineering and Computer Science (1974 to present), and Associate Dean of the College of Engineering (1982 to 1987; 1994 to present). He has published five books and over 150 papers in electromagnetic theory, antennas, microwaves, scattering, modern optics, and applied mathematics.

Dr. Uslenghi served as Secretary-Treasurer, Vice-Chair, and Chair of the Joint AP/MTT Chicago Chapter of IEEE twice, in 1975 to 1978 and 1989 to 1992. He was the General Chairperson of the 1992 AP-S International Symposium and URSI/NEM Meeting held in Chicago. He is a member of the AP-S AdCom, of the joint committee on future symposia of AP-S and USNC/URSI-B, the chair of the Technical Activities Committee of USNC/URSI-B, and the Vice-Chair Elect of Commission B of USNC/URSI. He is editor of the IEEE Transactions on Antennas and Propagation, the past editor of *Electromagnetics* and has served for many years on the editorial boards of the *Journal of Electromagnetic Waves and Applications*, the *European Journal of Telecommunications*, and *Alta Frequenza*. He is a member of Phi Beta Kappa, Sigma Xi, and Ursi Commissions B and D.